Using triple-layer remote phosphor structures LaVO₄:Eu³⁺ and ZnS:Cu,Sn to improve the chromatic uniformity and luminous quality of WLEDs

Phuc Dang Huu[1], Dieu An Nguyen Thi[2], Anh Minh D. Tran[3]
[1]Faculty of Fundamental Science, Industrial University of Ho Chi Minh City, Ho Chi Minh City, Vietnam
[2]Faculty of Electrical Engineering Technology, Industrial University of Ho Chi Minh, Ho Chi Minh City, Viet Nam
[3]Faculty of Electrical and Electronics Engineering, Ton Duc Thang University, Ho Chi Minh City, Vietnam

Article Info

ABSTRACT

This research paper investigates the novel triple remote phosphor layer for improving the remote phosphor's angular chroma uniformity (ACU) of down-light lamps by using remote micro-patterned phosphor layers (RMPP). In addition, introducing the triple-layer (TL) RMPP is introduced to offer the potential approach to this objective. This analysis also measures the optical efficiency of the layers and the angle distribution of angular correlated color temperature (ACCT). Drawing a comparison between the traditional dual-layer (DL) RMPP and the proposed TL is furthermore critical to this study. According to the findings, the triple-layer phosphor configuration can achieve greater hue consistency while having a correlating colour temperature (CCT) variance merely measured at 441 K. Results in the single RMPP layer are 1390 K of the remote phosphor (RP) sheet setting and 556 K for the ACCT deviation. The recreation employing finite-difference time-domain (FDTD) as well as the approach of ray-tracing ensures an increase in angular color uniformity (ACU). The structure of DL and TL RMPPs results in a 6.68 % and 4.69 % gain in luminous efficiency, respectively, with the standard RMPP layer at a currently driving of 350 mA. The micro-patterned layer's scattering characteristic and mixing effect may account for the increased ACU and luminous efficiency.

This is an open access article under the CC BY-SA license.

Corresponding Author:

Anh Minh D. Tran
Faculty of Electrical and Electronics Engineering, Ton Duc Thang University
Ho Chi Minh City, Vietnam
Email: tranducanhminh@tdtu.edu.vn

1. INTRODUCTION

Studies have demonstrated the outstanding photoluminescence quantum yields (PQYs), short emission full width at the half limit (FWHM), as well as tunability for discharge wavelengths for perovskite quantum dots (PQDs), making a way for the lead halide PQDs to be an ideal candidate for wide-gamut display applications [1]-[3]. Inorganic PQDs outperform organic-inorganic shielded PQDs in terms of stability and thus have attracted a massive interest as an essential material to down-convert lights from the chips of white light-emitting diodes (WLEDs) [4], [5]. However, critical enhancements in PQDs' optical performances and reliability, and cost efficiency are required to progress their practical applications. PQDs, in particular, have limited chemical and optical stability, which causes them to quickly degrade when exposed to moisture, heat, or light [6], [7]. As a result, PQDs show lower stability than traditional rare-earth phosphor types [8]. Several studies aimed at improving PQDs' robustness by having them coated in an organic-material layer such as CdS [9],

zeolite [10] glass [11], CaF_2 [12], Al_2O_3 [13], SiO_2 [14], and TiO_2 [15]. In general, using these inorganic materials to prepare the protective shells of PQDs in situ synthesis. Although with such protective coatings, the PQDs could obtain irradiation stabilities accompanying a high chemical and thermal shield, their water stability still needs further improvements. For example, after a 40-hour water-resistance test, the green PQD shielded with CaF_2 exhibited a drop in its luminescent strength to below 50% [16]. The method to obtain high water-stability PQDs is to get them incorporated into a confined matrix of organic polymer and glass [17]-[19]. This matrix was successful in forming a protective shield for the PQD core thanks to its thick polymer chains and hydrophobic surface, leading to a great improvement in its moisture stability (stable in water after a few months). However, this organic-matrix coating presented a limit in thermal conductivity, resulting in inefficient heat dispersion and stability; as a result, most polymer matrices have poor stability under ultraviolet (UV) excitation. These constraints restrict the utilization of the PQDs when it comes to LED chip incorporation [20], [21]. Besides, creating a merger between PQDs and different substances, for example, using nano-granules of Ag to transmute energy by plasmonic hot electrons or Fe_3O_4 nanoparticles for magnetic power, is gradually becoming an important topic to broaden their application range. We implement super hydrophobic aerogel inorganic matrices (shorten as "S-AIMs") with open layouts such as a water safety matrix as well as an integrating zone to contain lead halide PQDs to investigate the performance of highly water stable PQDs integrated into an ajar matrix. The PQDs can be easily embedded in the matrix through a simple post adsorption process, retaining their luminescence properties while providing superior water stability. Then, the PQDs combined with the S-AIM (AeroPQDs) are applied to WLEDs for integration tests. Finally, thanks to the open structure, the other functional nanomaterials, suchlike Fe_3O_4 nanoparticles, can incorporate into AeroPQDs. They have enormous potential for being a foundational fluorescence-integrating platform with excellent stability for functional material compounds, which will broaden the range of applications for PQDs.

2. PREPARATION

This research suggests using a monoclinic structured phosphor $LaVO_4:Eu^{3+}$. Before the process, be sure to prepare the required compositions as Table 1. Initially, all ingredients are blended uniformly by grinding or milling. Then, burning them in open quartz boats under a temperature of 900 °C for an hour. Next, pulverize the mixture. The second step is to heat them for another hour in unshielded quartz boats, and the temperature this time is 1100 °C. Later, grind them into powder. After being washed in a NaOH (or KOH) solution in water followed by multiple instances of washing in plain water, the mixture is left dried. In the end, fire the mixture within open quartz boats for an hour under 1100 °C. The light attributes of the outcome product must have the emission color of red, emission peak range from 1.773 eV to 2.115 eV. Plus, the excitation efficacy by UV is ++(4.88 eV), +(3.40 eV) [22].

Table 1. Chemical components of $LaVO_4:Eu^{3+}$ phosphor with red emission

Ingredients	Mole %	By weight (g)
La_2O_3	95 (of La)	155
Eu_2O_3	5 (of Eu)	8.8
NH_4VO_3	110	129

Table 2. Components for ZnS:Cu,Sn with green emission

Ingredients	Mole %	By weight (g)
Y_2O_3	80 (of Y)	90.4
CeO_2	10	17.2
Tb_4O_7	10 (of Tb)	18.7
Al_2O_3	300 (of Al)	153
H_3BO_3	410	254

Another phosphor in this study is hexagonal (wurtzite) phosphor ZnS:Cu,Sn with Table 2. First, dissolving the copper acetate via a small amount of water, put the solution in the blend of ZnS and SnS. Next, create a slurry using water or methanol. Let dry and then pulverize the mixture. Later, put in sulfur (about 2 g −3 g). Finally, burn them within sealed quartz pipes with N_2 for an hour under 1150 °C. The light attributes should obtain the emission color of green that peaks at 2.41 eV, and 0.32-eV emission width, as well as the excitation efficiency by UV of ++(4.88 eV), +(3.40 eV) [23].

The schematic design depicts a cross-section of the LEDs kit under investigation in Figure 1. In addition, Figure 1(a) and Figure 1(b) individually show the form information for a remote-dome, a remote-plate, a half-dome, and a conformal-coating pc-WLED layout. The blue square represents the LED chips, the phosphor layer indicates by the yellow stripes, and the silicone matrix lenses by the blank zones. Aluminum nitride is assumed to create the substrate, whereas $YAG:Ce^{3+}$ ought to be the phosphor. When viewed along the z-axis, all of the CCTs in each structure setting to 6500 K.
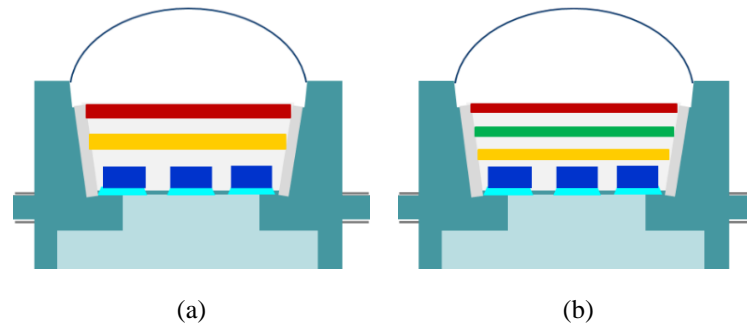
(a)   (b)

Figure 1. Illustration of (a) double-sheet phosphor (DL) and (b) three-sheet phosphor (TL) structures

The breadth for these phosphor layers will be 0.08 mm. Furthermore, the concentration for YAG:Ce3+ varies in response to shifts in the red and green phosphor concentrations to preserve the average color-associated temperature (or average CCT). Besides, the YAG:Ce3+ concentrations vary depending on the average CCT (ACCT) of each phosphor structure, resulting in a broad array of scattering characteristics within WLEDs. This disparity consequently results in variations in optical properties.

Figure 2 shows that the yellow YAG:Ce3+ phosphor concentration exhibited by two remote micro-patterned phosphor layers (RMPP) structures decreases as the ACCT is higher. Notably, triple-layer (TL) shows a much more significant decline of YAG:Ce3+ concentration than the dual-layer (DL) exhibits. The high concentration of YAG:Ce3+ concentrations are known as one of the main reasons for excessive backscattering event and thermal instability in a WLED's performance. Specifically, considering the same ACCT in all systems, back-scattering will occur more if the system has greater YAG:Ce3+ content, causing a severe reduction for the released luminous flux [24], [25]. Moreover, when the concentration of YAG:Ce3+ increases, the balance among the key hues essential for white light production, containing yellow, red, and green, would be diminished, resulting in a loss of color quality. As a result, by boosting the red spectral intensity with red-emitting materials, the back-scattering has been minimized to stimulate the lighting extraction and coloration efficiencies of a WLED. Furthermore, the green light can regulate chromatic uniformity and luminous flux. For handling optical properties regarding essential factors, the TL that uses both green and red phosphor films seems to be a more promising candidate. The research team continuously investigate other references to remote phosphor structures and emission spectra, as shown in Figure 3.
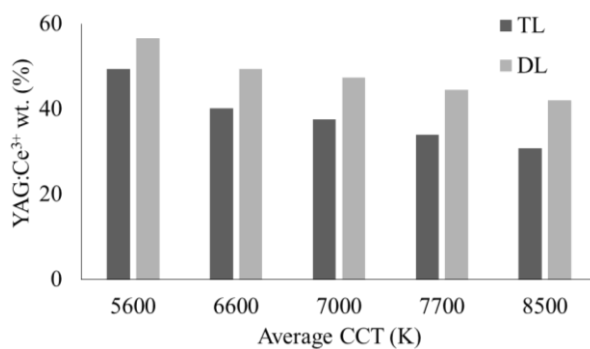

Figure 2. The concentration for YAG:Ce^{3+} phosphor in two RMPP structures: TL and DL under various ACCT values
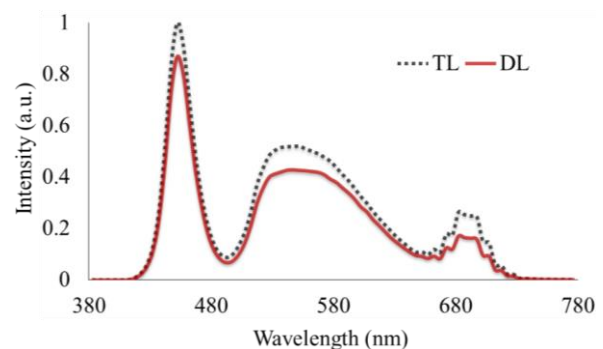
Figure 3. Discharge spectra for two RMPP structures: TL and DL

3. RESULTS AND DISCUSSION

The color rendering index (CRI) comparison between the remote phosphor configurations is shown in Figure 4. Regardless of ACCT, the DL RMPP has the highest CRI which grows gradually as ACCT values become larger. The peak CRI is observed at up to 73 when the ACCT is 8500 K. With a high ACCT of 8500 K, acquiring enhancement in CRI is relatively challenging; however, according to this result, using the DL RMPP is a promising approach to CRI improvement. It is the red-light supplement from LaVO$_4$:Eu^{3+} phosphor sheet that helps improve the CRI. In terms of CRI, the TL structure has a slightly lower performance than the DL. As a result, it is trustworthy to assume that, with CRI as the target, the yellow-red (YR) structure seems promising in mass-production WLEDs. CRI, on the other hand, is just one of the color

quality indices. Many researchers have recently been interested in a parameter known as color quality scale (CQS). The sum of three factors is CQS:CRI, viewer preference, and chromaticity coordinate. CQS has become a substantial target of researchers due to its coverage of these three variables, and it appears to be the most critical way to test chromaticity. Figure 5 of this analysis compares the CQS of DL and TL RMPP structures. Because of the equilibrium among the hues of yellow, yellow, green, and red, the TL achieves a more significant CQS. Notably, the color adequacy can rise along with the CQS. The CQS, on the other hand, gets lower values in the DL RMPP package. Generally, that the TL structure could benefit the CQS and color adequacy greatly depends on the applied red and green phosphor films, which significantly contribute to adding more red and green light components.
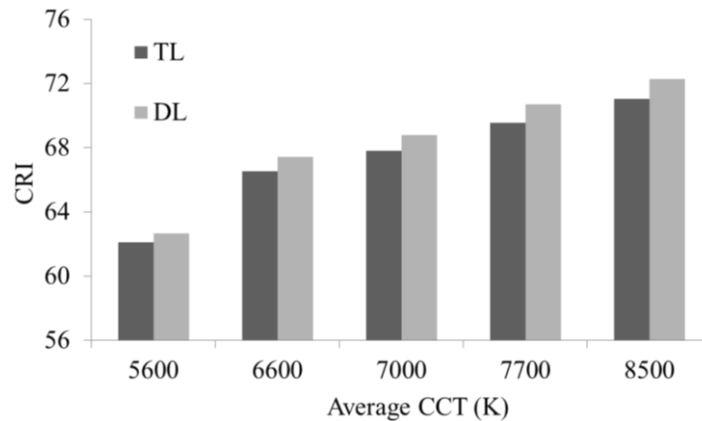

Figure 4. CRIs of two RMPP structures: TL and DL at different ACCTs

Figure 5 shows that if color quality is a priority for manufacturers, they should opt for the TL structure. If the luminous output is affected, can the chromatic performance improve? the research group examined the emitted lumen in single-layer (SL) as well as DL RMPP structures. This section describes and explains the blue-light transmittance's and yellow-light conversion's computations in the DL RMPP to examine the stimulation in LED efficiency achieved by this structure.
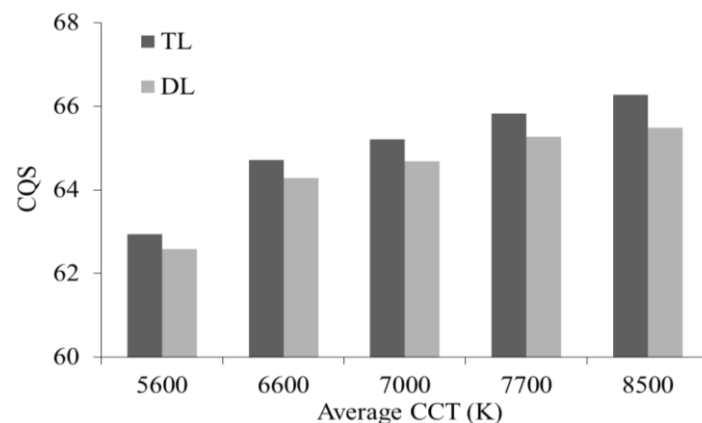

Figure 5. CQS of two RMPP structures: TL and DL at different ACCTs

The data in Figure 6 has demonstrated that applying several phosphor layers improves the luminous flux more than just one. Based on this finding, the TL RMPP structure displays a higher luminous output (LO) than the DL RMPP does, as in Figure 6. This result together with the outstanding CQS, demonstrated by the TL, has dispelled the doubts about the advantages of acquiring LO enhancement using this RMPP structure. The benefits performed on LO can be thanks to the green phosphor layer ZnS:Cu,Sn. Particularly, the green ZnS:Cu,Sn phosphor layer boosts the green light portion and broadens the emission spectrum in the

500 nm – 600 nm wavelength range. Also, in this range, the emission strength of TL is higher than DL, since its YAG:Ce^{3+} phosphor concentration is the lowest to maintain the ACCT. The TL structure will then minimize internal backscattering, letting LED-chip emitted blue illumination bypassing the closest phosphor sheet (YAG:Ce^{3+} sheet) to reach the other layers. In other words, the TL RMPP aids in the efficient energy conversion of blue lights pumped by a LED-chip cluster. Consequently, the discharge spectrum strength from the TL appears to be the strongest, resulting in the best improvement in the exhibited LO. As a result, the TL RMPP package is a potential alternative because it has better optical properties than other WLED structures, such as CQS and LO.
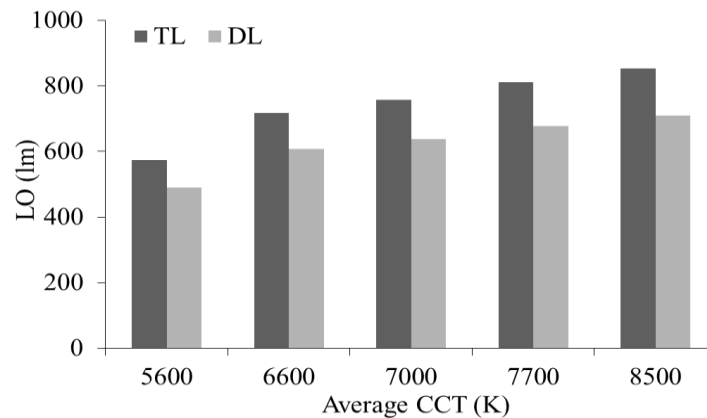

Figure 6. LO of two RMPP structures: TL and DL at different ACCT values

Regardless, chromatic uniformity is one of the most critical aspects of color consistency. Certain techniques are available for improving hue consistency, such as utilizing phosphor granules (SiO$_2$, CaCO$_3$, ec.) to increase forward-scatterings, or using a conformal phosphor structure [26]. While these two methods increase color uniformity, the luminous flux appears to be decreasing. Furthermore, using the green ZnS:Cu,Sn phosphor and the red LaVO$_4$:Eu^{3+} phosphor can increase both the scattering properties and the red as well as green illumination presence within WLEDs, yielding a superior white illumination generation. Additionally, to reduce backscatterings to the LED chips, using the RMPP design will boost the LO of the whole WLED device. The Lambert-Beer law in equation 6 suggests changing the phosphor concentration to a sufficient level to obtain the maximum power transmission. The comparison of color deviation among the structures is in Figure 7. Nevertheless, the rise in either backward or forward-scattering can cause a drop in the LO. This argument can be shown by the effect of increasing scattering in the WLED package when more phosphor films are added: the emitted light with essential color components can be scattered and distributed at wider angles, leading to better color blending. Therefore, WLEDs' chromatic uniformity improves.
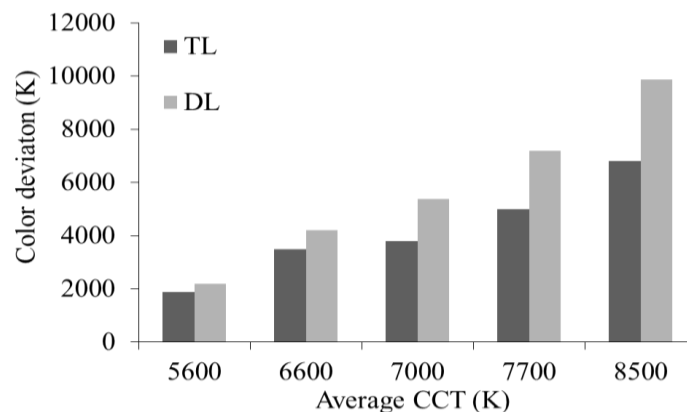

Figure 7. Hue aberration in two RMPP structures: TL and DL at different ACCTs

4. CONCLUSION

The comparison between the performances of two RMPP packages, the TL and DL, is drawn in this paper. During the simulation, the packages are investigated at five ACCT points with the use of the green ZnS:Cu, Sn and red $LaVO_4$:Eu^{3+} phosphors. Both the Mie principle and the Lambert-Beer rule back up the study findings. According to the findings, the addition of a green ZnS:Cu,Sn phosphor layer improves the green light portion, resulting in improved angular color uniformity (CU) and LO. Hence, the TL RMPP has more significant LO and CU than the DL structure. Besides, increasing the red-light portion by using a red $LaVO_4$:Eu^{3+} phosphor layer will boost the CRI and CQS. The TL structure also has a higher CQS but a lower CRI than the DL structure. The primary hues' proportions: yellow, red, as well as green, determine the chromaticity. As a result, the TL proves to be the best option for manipulating these three colors. Additionally, the TL structure's luminous flux clearly increases as backscattering reduces. The fact that TL has the highest luminous efficiency value is evidence enough. By taking this paper as a critical reference, the manufacturer may find it possible and easy to select the most suitable RMPP model to improve the WLED optical adequacies.

REFERENCES

[1] C. Bai *et al.*, "Full-color optically-sectioned imaging by wide-field microscopy via deep-learning," *Biomedical Optics Express*, vol. 11, no. 6, pp. 2619-2632, 2020, doi: 10.1364/BOE.389852.
[2] Z. Zhang dan W. Yang, "Tunable photoluminescence in Ba1-xSrxSi3O4N2: Eu2+/ Ce3+, Li+ solid solution phosphors induced by linear structural evolution," *Optical Materials Express*, vol. 9, no. 4, pp. 1922-1932, 2019, doi: 10.1364/OME.9.001922.
[3] T. Y. Orudzhev, S. G. Abullaeva, and R. B. Dzhabbrov, "Increasing the extraction efficiency of a light-emitting diode using a pyramid-like phosphor layer," *Journal of Optical Technology*, vol. 86, no. 10, pp. 671-676, 2019, doi: 10.1364/JOT.86.000671.
[4] L. Li, Y. Zhou, F. Qin, Y. Zheng, and Z. Zhang, "On the Er3+ NIR photoluminescence at 800 nm," *Optics Express*, vol. 28, no. 3, pp. 3995-4000, 2020, doi: 10.1364/OE.386792.
[5] A. Zhang *et al.,* "Tunable white light emission of a large area film-forming macromolecular complex with a high color rendering index," *Optical Materials Express*, vol. 8, no. 12, pp. 3635-3652, 2018, doi: 10.1364/OME.8.003635.
[6] X. Hu *et al.,* "Optimizing selection of the test color sample set for the CIE 2017 color fidelity index," *Optics Express*, vol. 28, no. 6, pp. 8407-8422, 2020, doi: 10.1364/OE.383283.
[7] A. Udupa, X. Yu, L. Edwards, and L. L. Goddard, "Selective area formation of arsenic oxide-rich octahedral microcrystals during photochemical etching of n-type GaAs," *Optical Materials Express*, vol. 8, no. 2, pp. 289-294, 2018, doi: 10.1364/OME.8.000289.
[8] M. M. M. -Canto, L. I. W. McKinna, B. J. Robson, and K. E. Febricius, "Model for deriving benthic irradiance in the Great Barrier Reef from MODIS satellite imagery," *Optics Express*, vol. 27, no. 20, pp. A1350-A1371, 2019, doi: 10.1364/OE.27.0A1350.
[9] I. G. Palchikova, E. S. Smirnov, and E. Iv. Palchikov, "Quantization noise as a determinant for color thresholds in machine vision," *Journal of the Optical Society of America A*, vol. 35, no. 4, pp. B214-B222, 2018, doi: 10.1364/JOSAA.35.00B214.
[10] T. Kozacki, M. Chlipala, and H. -G. Choo, "Fourier rainbow holography," *Optics Express*, vol. 26, no. 19, pp. 25086-25097, 2018, doi: 10.1364/OE.26.025086.
[11] S. -W. Jeon, S. Kim, J. Choi, I. Jang, Y. Song, H. W. Kim, and J. P. Kim, "Optical design of dental light using a remote phosphor light-emitting diode package for improving illumination uniformity," *Applied Optics*, vol. 57, no. 21, pp. 5998-6003, 2018, doi: 10.1364/AO.57.005998.
[12] Y. -T. Wang *et al.,* "Color conversion efficiency enhancement of colloidal quantum dot through its linkage with synthesized metal nanoparticle on a blue light-emitting diode," *Optics Letters*, vol. 44, no. 23, pp. 5691-5694, 2019, doi: 10.1364/OL.44.005691.
[13] Y. Tang, Z. Li, G. Liang, Z. Li, J. Li, and B. Yu," Enhancement of luminous efficacy for LED lamps by introducing polyacrylonitrile electrospinning nanofiber film," *Optics Express*, vol. 26, no. 21, pp. 27716-27725, 2018, doi: 10.1364/OE.26.027716.
[14] P. Zhu, H. Zhu, G. C. Adhikari, and S. Thapa, "Design of circadian white light-emitting diodes with tunable color temperature and nearly perfect color rendition," *OSA Continuum*, vol. 2, no. 8, pp. 2413-2427, 2019, doi: 10.1364/OSAC.2.002413.
[15] A. J. Henning, J. Williamson, H. Martin, and X. Jiang, "Improvements to dispersed reference interferometry: beyond the linear approximation," *Applied Optics*, vol. 58, no. 1, pp. 131-136, 2019, doi: 10.1364/AO.58.000131.
[16] C. Zhang, T. Han, S. Cao, X. Cheng, and J. Zhang, "Mn4+-doped fluoride phosphors rapidly synthesized by ball milling," *Optical Materials Express*, vol. 8, no. 1, pp. 73-81, 2018, doi: 10.1364/OME.8.000073.
[17] X. Bao, X. Gu, and W. Zhang, "User-centric quality of experience optimized resource allocation algorithm in VLC network with multi-color LED," *Optics Express*, vol. 26, no. 21, pp. 27826-27841, 2018, doi: 10.1364/OE.26.027826.
[18] J. Cheng *et al.*, "Luminescence and energy transfer properties of color-tunable Sr4La , PO4.3O: Ce3+, Tb3+, Mn2+ phosphors for WLEDs," *Optical Materials Express*, vol. 8, no. 7, pp. 1850-1862, 2018, doi: 10.1364/OME.8.001850.
[19] X. Yuan *et al.*, "Ultra-high capacity for three-dimensional optical data storage inside transparent fluorescent tape," *Optics Letters*, vol. 45, no. 6, pp. 1535-1538, 2020, doi: 10.1364/OL.387278.
[20] W. Wang and P. Zhu, "Red photoluminescent Eu3+-doped Y2O3 nanospheres for LED-phosphor applications: Synthesis and characterization," *Optics Express*, vol. 26, no. 26, pp. 34820-34829, 2018, doi: 10.1364/OE.26.034820.
[21] P. Kumar and N. K. Nishchal, "Enhanced exclusive-OR and quick response code-based image encryption through incoherent illumination," *Applied Optics*, vol. 58, no. 6, pp. 1408-1412, 2019, doi: 10.1364/AO.58.001408.
[22] A. Motazedifard, S. Dehbod, and A. Salehpour, "Measurement of thickness of thin film by fitting to the intensity profile of Fresnel diffraction from a nanophase step," *Journal of the Optical Society of America A*, vol. 35, no. 12, pp. 2010-2019, 2018, doi: 10.1364/JOSAA.35.002010.
[23] R. E. O'Shea, S. R. Laney, and Z. Lee, "Evaluation of glint correction approaches for fine-scale ocean color measurements by lightweight hyperspectral imaging spectrometers," *Applied Optics*, vol. 59, no. 7, pp. B18-B34, 2020, doi: 10.1364/AO.377059.

[24] Y. Xie *et al*., "Encapsulated room-temperature synthesized CsPbX3 perovskite quantum dots with high stability and wide color gamut for display," *Optical Materials Express*, vol. 8, no. 11, pp. 3494-3505, 2018, doi: 10.1364/OME.8.003494.
[25] L. Duan and Z. Lei, "Wide color gamut display with white and emerald backlighting," *Applied Optics*, vol. 57, no. 6, pp. 1338-1344, 2018, doi: 10.1364/AO.57.001338.
[26] Y. L. Piao, M. -U. Erdenebat, K. -C. Kwon, S. -K. Gil and N. Kim, "Chromatic-dispersion-corrected full-color holographic display using directional-view image scaling method," *Applied Optics,* vol. 58, no. 5, pp. A120-A127, 2019, doi: 10.1364/AO.58.00A120.

BIOGRAPHIES OF AUTHORS

Phuc Dang Huu received a Physics Ph. D degree from the University of Science, Ho Chi Minh City, in 2018. Currently, he is a lecturer at the Faculty of Fundamental Science, Industrial University of Ho Chi Minh City, Ho Chi Minh City, Vietnam. His research interests include simulation LEDs material, renewable energy. He can be contacted at email: danghuuphuc@iuh.edu.vn.

Dieu An Nguyen Thi received a master of Electrical Engineering, HCMC University of Technology and Education, VietNam. Currently, she is a lecturer at the Faculty of Electrical Engineering Technology, Industrial University of Ho Chi Minh City, Viet Nam. Her research interests are Theoretical Physics and Mathematical Physics. She can be contacted at email: nguyenthidieuan@iuh.edu.vn.

Anh Minh D. Tran got his B.S. and M.S. degrees in Control and Automation Engineering from Ho Chi Minh City University of Transport in 2008 and Ho Chi Minh University of Technology in 2013, respectively, and his Ph.D. from Pukyong National University in Busan, Korea, in 2017. He is currently a lecturer at the Faculty of Electrical and Electronics Engineering at Ton Duc Thang University in Ho Chi Minh City, Vietnam. His scientific interests include control theory, computer vision, and optical science with applications to industry and the environment. He can be contacted at email: tranducanhminh@tdtu.edu.vn.